Supporting Information for

Controlled Fractal Growth of Transition Metal Dichalcogenides

Peijian Wang,[†,‡,⊥] Siyuan Luo,[‖,‡,⊥] Lincoln Boyle,[‡] Shaoming Huang,[†] Hao Zeng[‡,*]

†School of Materials and Energy, Guangdong University of Technology, Guangzhou Higher Education Mega Center, Panyu District, Guangzhou, 510006, China
‖Key Laboratory for Thin Film and Microfabrication of Ministry of Education, School of Electronic Information and Electrical Engineering, Shanghai Jiao Tong University, Shanghai, 200240, China
‡Department of Physics, SUNY-Buffalo, Buffalo, NY, 14260, United States

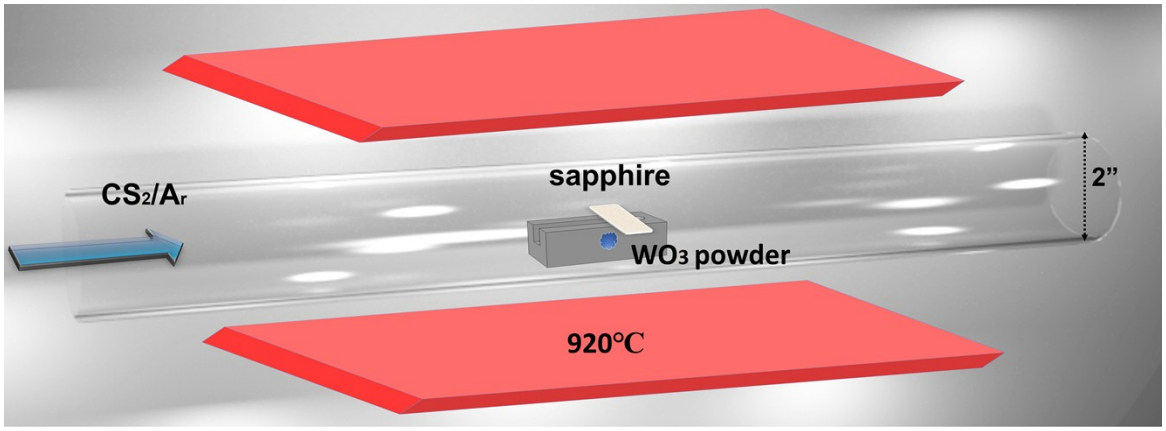

Figure S1. Schematic for the CVD set up. The CS_2 carried by argon gas was used as the sulfur source. The sapphire substrate, supported by the graphite boat, was facing toward the WO_3 powder.

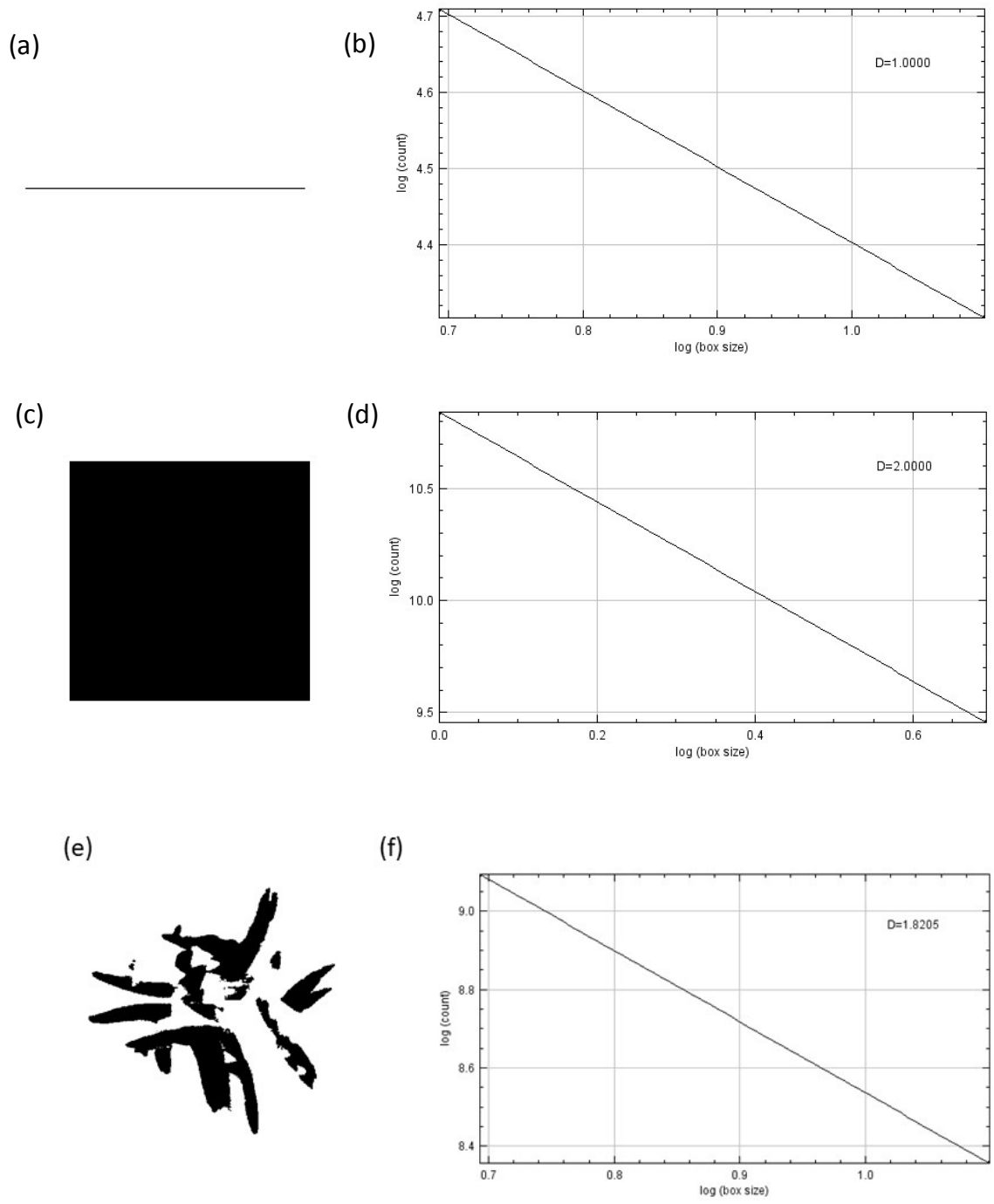

Figure S2. (a)(b) Fractal dimension by box counting method reveals that the fractal dimension for a line is 1. (c)(d) Fractal dimension by box counting method reveals that the fractal dimension for a square is 2. (e)(f) Fractal dimension by box counting method of a fractal feature shows it has a fractal dimension of 1.8205.

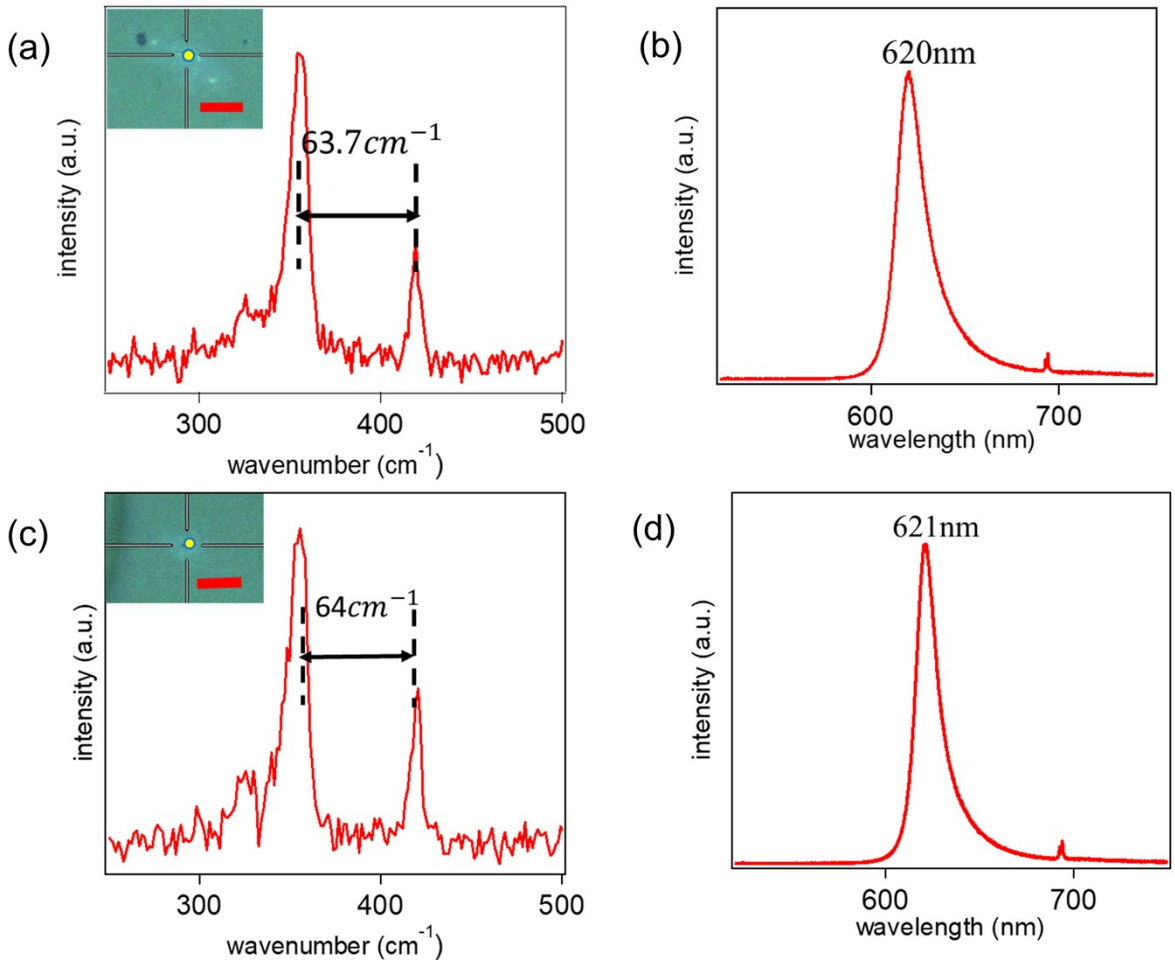

Figure S3. (a) (c) Raman spectrum measured at aggregates formed in early growth stage, by opening lid after 2 mins' growth, the less than 65 cm^{-1} wavenumber difference revealing it is monolayer.[1-2] The insets show the position of measurements. Scale bars are all 10um. (b) (d) Corresponding PL measurements taken at the spots in insets in (a)(c), the peak positions are in agreement with the references.[1]

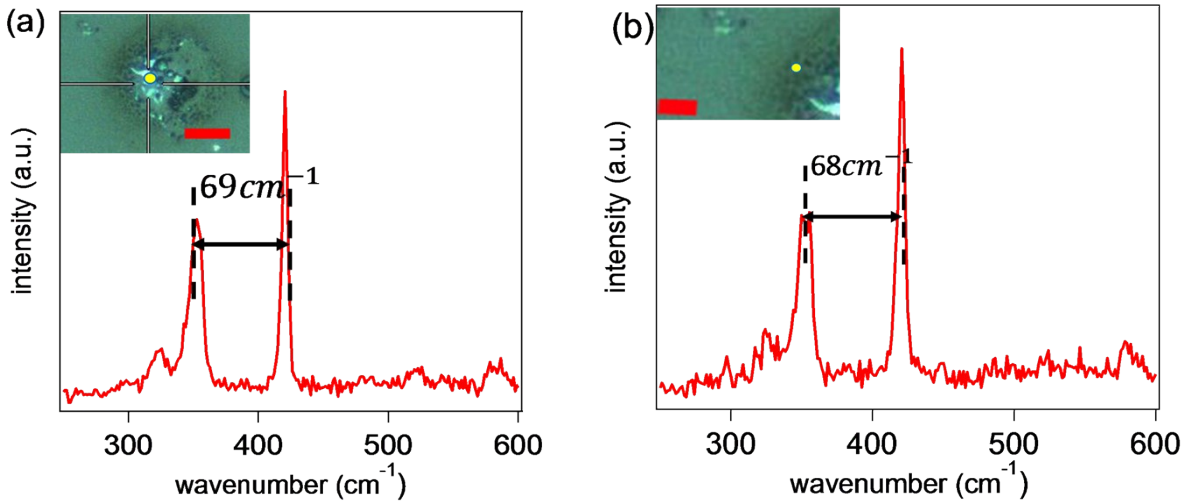

Figure S4. (a) Raman spectrum on the cluster of WS_2 after 1min's growth, showing a wavenumber difference of 69 cm^{-1} between E_{2g} and A_{1g}. Inset displays the optical microscopic image of the WS_2 cluster. (b) Raman spectrum on the feature of WS_2 after 1min's growth. The 68 cm^{-1}, wavenumber difference between E_{2g} and A_{1g}, shows it is thinner than the interior cluster. The scale bars are 5um.

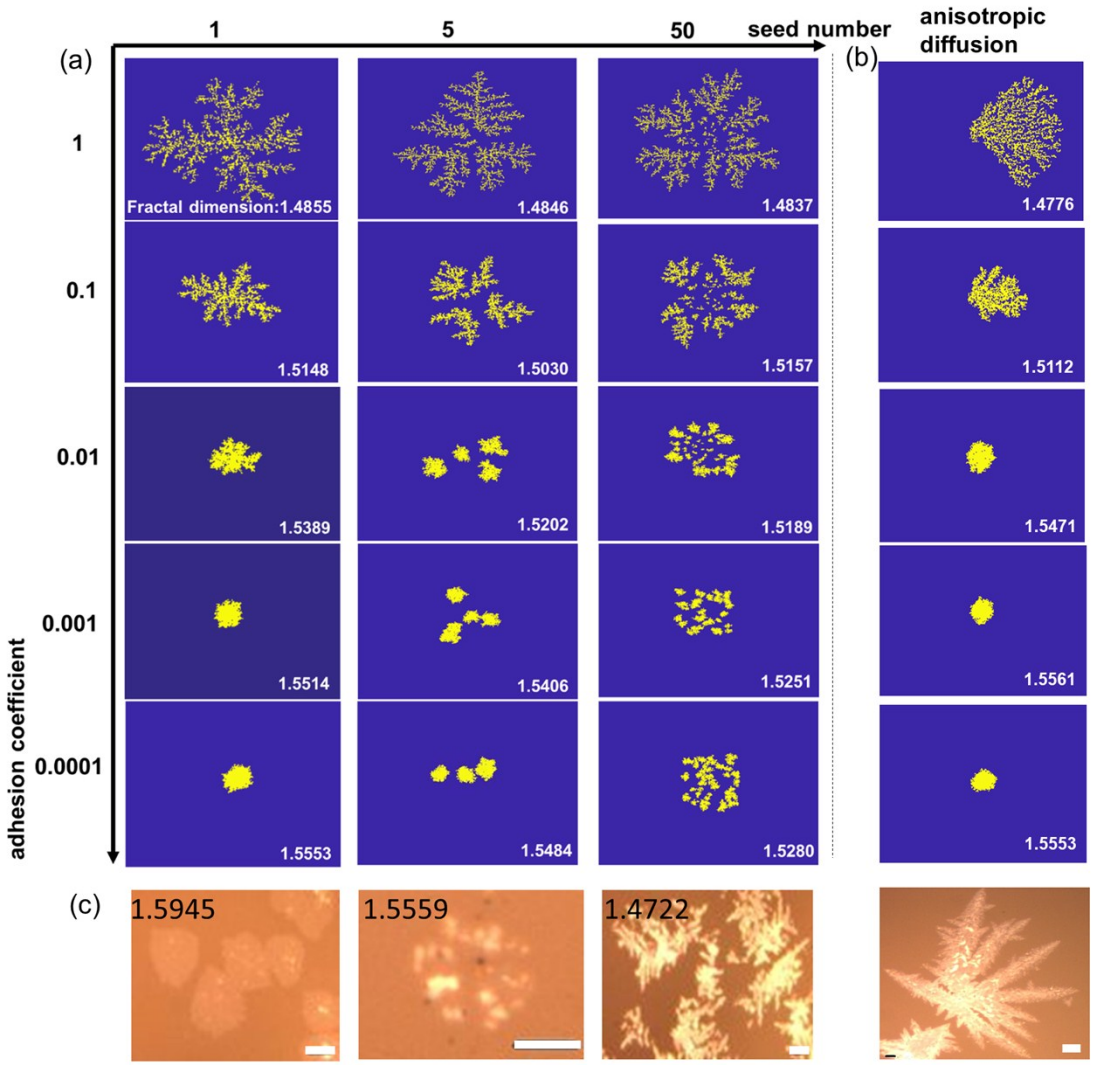

Figure S5. (a) The simulation results by DLA algorithm, displaying evolution with different seed numbers and adhesion coefficients. The ratio of occupied site pixel number/total pixel number of all frames is the same: 0.041. Seed number in columns from left to right: 1, 5, 50. The adhesion coefficients from top to bottom: 1, 0.1, 0.01, 0.001, 0.0001. The white number in each frame indicates the fractal dimension of the dendritic structure in the frame. (b) The simulation results of anisotropic diffusion. The probability of going to the right is 0.3, to the left is 0.2, and up and down are both 0.25. The ratio of occupied site pixel number/total pixel number of all frames is the same: 0.041. When the adhesion coefficient is low, the results become less anisotropic, resembling the "cloud-like" features. (c) Some microscopic images found in the growth. In the first image, the "cloud-like" feature resemble the last two images in single seed column with low adhesion coefficient. The cluster in the second image resembles the last three images in the 50 seeds column with low adhesion coefficient results. The third image is the dendritic feature, which resemble the simulation results when the adhesion coefficient is high. In the fourth image, the "bloom-like" feature resemble the first image of the simulation of the anisotropic diffusion in (b). The scale bars are all 5um.

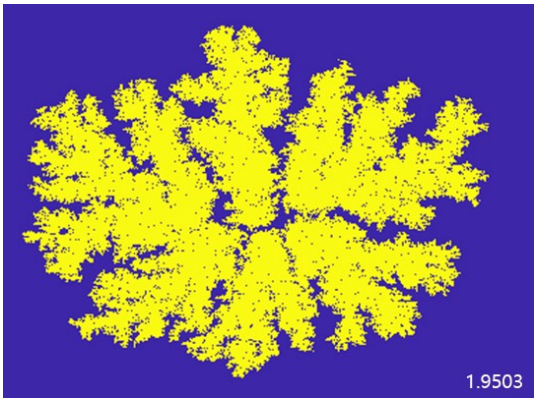

Figure S6. The result of simulation of 1-hour DLA growth in which the seed number is 1 and step number is 60×10^8. The lower-right value displays the fractal dimension.

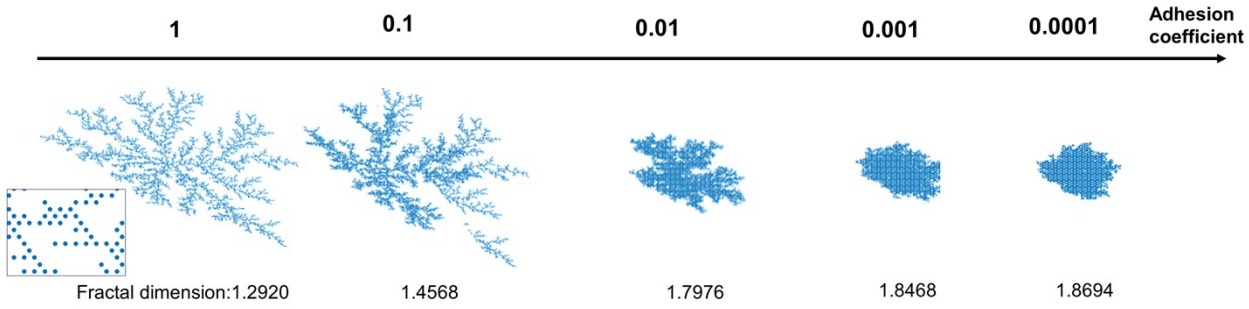

Figure S7. The result of simulation of DLA growth in hexagonal lattice, with different adhesion coefficient. The seed number is 1. The fractal dimensions are indicated on the bottom. The fractal dimension increases with the adhesion coefficients decreases. The inset is the magnification of the simulation result (adhesion coefficient=1), showing the lattice symmetry. The ratio of occupied pixel number/total pixel number is the same for the images: 0.041.

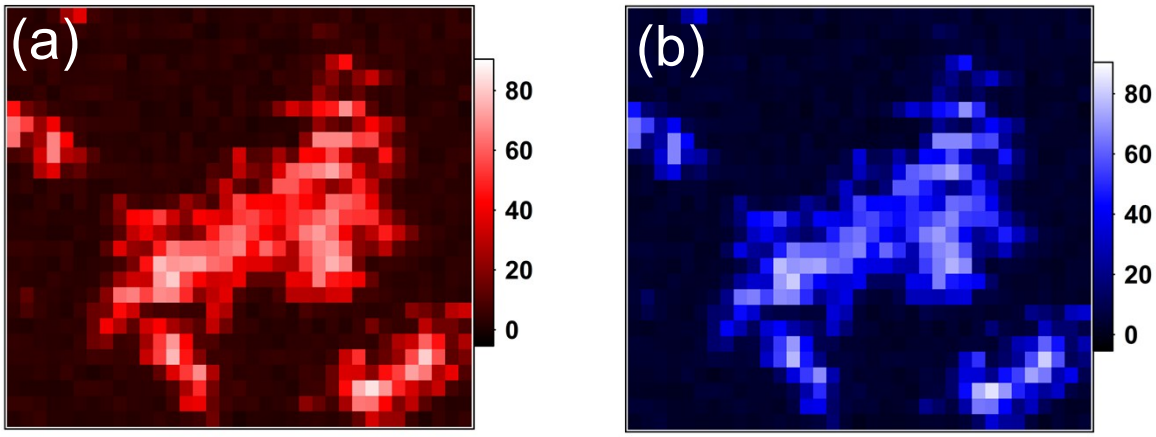

Figure S8. (a) Raman intensity map of a dendrite at wavenumber of 354 cm^{-1}. (b) Raman intensity map of the a dendrite at wavenumber of 419 cm^{-1}.

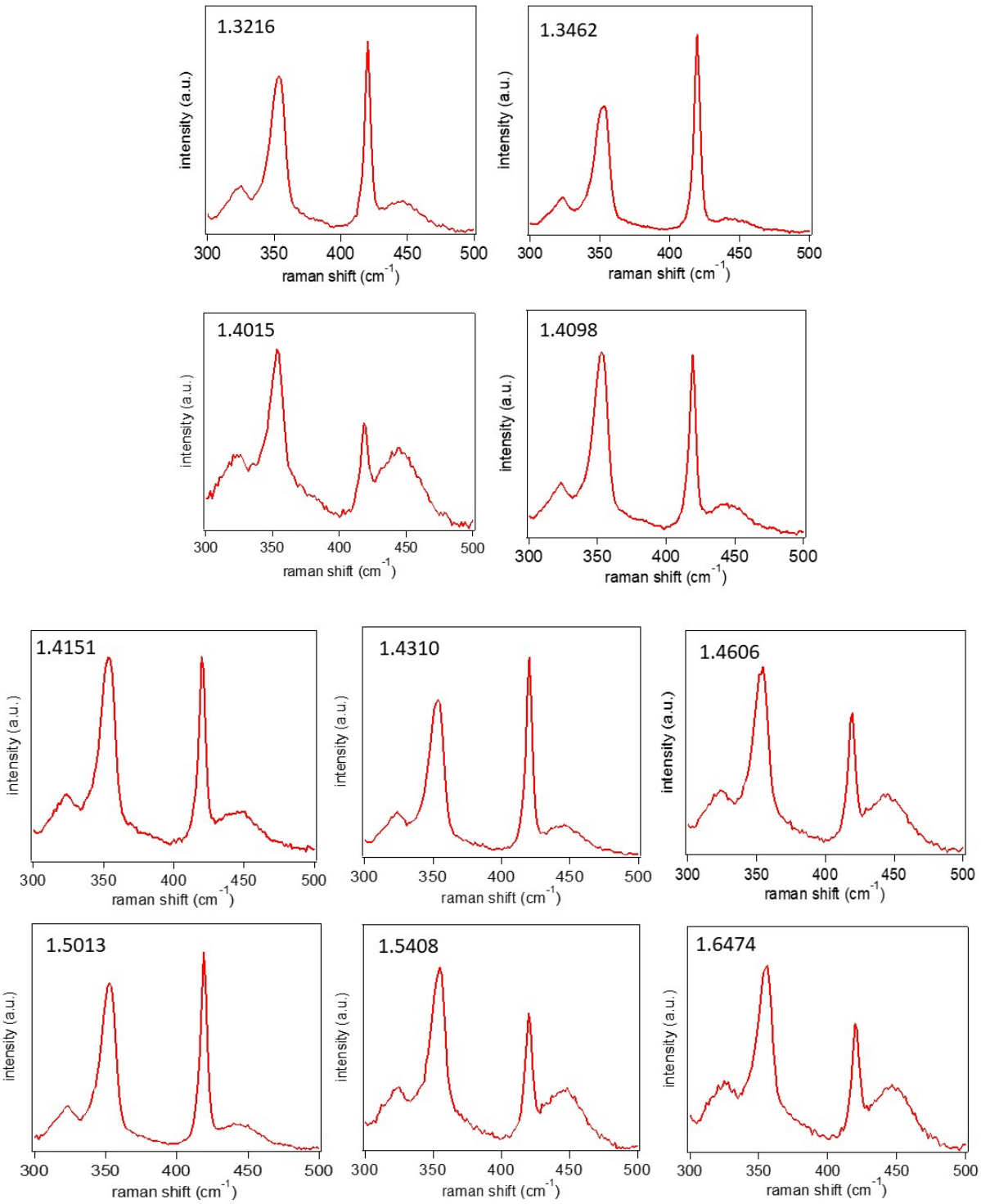

Figure S9. Raman spectra of the fractal monolayers with different fractal dimension in Figure 5d.

Reference

1. Zeng, H.; Liu, G. B.; Dai, J.; Yan, Y.; Zhu, B.; He, R.; Xie, L.; Xu, S.; Chen, X.; Cui, X.; et.al.;, Optical Signature of Symmetry Variations and Spin-Valley Coupling in Atomically Thin Tungsten Dichalcogenides. *Scientific Reports* **2013,** *3*, 1-5.
2. Withers, F.; Bointon, T. H.; Huadson, D. C.; Craciun, M. F.; Russo, S., Electron Transport of WS2 Transistors in a Hexagonal Boron Nitride Dielectric Environment. *Scientific Reports* **2014,** *4*, 1-5.